

1 **Network inefficiency - Empirical findings for six**
2 **European cities**

3 **Lisa S. Hamm***

4 Chair of Traffic Engineering and Control, TU Munich

5 DE-80333, Germany

6 Email: lisa.hamm@tum.de

7 **Allister Loder**

8 Chair of Traffic Engineering and Control, TU Munich

9 DE-80333, Germany

10 Email: allister.loder@tum.de

11 **Gabriel Tilg**

12 Chair of Traffic Engineering and Control, TU Munich

13 DE-80333, Germany

14 Email: gabriel.tilg@tum.de

15 **Monica Menendez**

16 Division of Engineering, NYU Abu Dhabi, UAE

17 Email: monica.menendez@nyu.edu

18 **Klaus Bogenberger**

19 Chair of Traffic Engineering and Control, TU Munich

20 DE-80333, Germany

21 Email: klaus.bogenberger@tum.de

22 * Corresponding author

23 Word count: 5646 words + 3 table(s) \times 250 = 7146 words

24

25 *Submitted:* December 6, 2021

26

27 Paper re-submitted for review at the Transportation Research Record

1 **ABSTRACT**

2 When planning road networks, inhomogeneous traffic conditions and the effects of multi-modal
3 interactions are often neglected. This can lead to a substantial overestimation of network capacities.
4 Empirical macroscopic fundamental diagrams or volume delay relationships show considerable
5 scatter, reflecting a reduction in network performance and an inefficient use of infrastructure. The
6 implication is that the external costs of vehicular (car) traffic get underestimated, when planning
7 traffic capacities and speeds based on optimal rather than on real estimates. In this paper, we
8 contribute with an explorative and empirical approach to analyze network inefficiency and quantify
9 its drivers. We propose to measure network efficiency by introducing the idea of excess delays
10 for the macroscopic fundamental diagram. We define excess delays as the difference between
11 the observed speed and the optimal network speed at a given density. We apply the concept on
12 traffic data sets of six European cities that differ in the data collection method and use quantile
13 regression methods for analysis. We find that excess delays are present in every data set and
14 increase with the road network's traffic load. We further confirm the intuition that traffic signal
15 control, network loading, and multimodality influence the level of network inefficiency. The excess
16 delay formula allows quantifying this information in a simple way and provides additional insights
17 apart from the standard MFD model. The approach supports planners to obtain better real-world
18 and less optimistic speed predictions for traffic analyses and suggests shifting urban transport to
19 more spatial and temporal efficient modes.

20 *Keywords:* macroscopic fundamental diagram, multi-modal, network efficiency, urban congestion,
21 policy

1 INTRODUCTION

2 We plan our road networks based on guidelines assuming normal and homogeneous traffic condi-
3 tions, not accounting for multi-modal interactions, and therefore an overestimation of capacities.
4 This results in rather best-case estimates of road traffic. Cost-benefit analyses may only consider
5 these best-case estimates, but lack information on some of the factors that can negatively affect net-
6 work performance, which, in turn, potentially alter planning decisions. Such negative effects are
7 observed everywhere in the unpredictable reality: empirical macroscopic fundamental diagrams or
8 volume delay relationships show considerable scatter, implying a reduction in performance and in-
9 efficient use of infrastructure (1, 2, 3, 4, 5). In urban road networks, the literature suggests at least
10 three sources contributing to inefficient infrastructure use: (i) interaction effects between different
11 vehicles types, (ii) traffic dynamics, and (iii) traffic control strategies. The implication is that when
12 cities plan and manage traffic capacities and speeds based on an optimal rather than on the real
13 estimates, the external costs of vehicular (car) traffic get underestimated.

14 In this paper, we contribute with an explorative and empirical approach to analyze network
15 inefficiency and quantify its drivers. We propose to measure network efficiency by introducing the
16 idea of excess delays for the macroscopic fundamental diagram (MFD). Excess delays add up to
17 inherent delays of traffic. The latter ones are already described by the MFD (6, 7) and fundamental
18 diagram. In this paper, we define the original MFD as *idealized*, i.e. as the maximum flow for
19 each density independently from demand. In contrast, the *observed* MFD is what we observe from
20 empirical or simulation data, and includes multi-modal interactions and demand-related effects.
21 Excess delays are the difference between both MFDs for a given density. More specifically, for a
22 certain density, we compare the speed, measured in units of pace, derived from the idealized and
23 the observed MFD. The excess delay approach allows quantifying the effects of signal control,
24 network loading, and multimodality on urban traffic in a simple way. Furthermore, it provides
25 additional insights such as the possibility to facilitate the modeling of hysteresis patterns in the
26 MFD.

27 Based on this procedure, we can measure excess delays for four real-world loop detector
28 data sets, one drone data set, and one simulation-based data set. We find that excess delays are
29 present in every data set and that they increase with the road network's traffic load. We find also
30 that there is a difference between the network loading and unloading dynamics, and that there
31 exists an intuitive influence of traffic signal control and multimodality on network inefficiency.
32 Interestingly, the estimates of all six sources are comparable, even though the data sets differ in
33 the collection method and the underlying network sizes, suggesting the global applicability of the
34 quantitative results of this analysis. The proposed approach of network inefficiency and excess
35 delays helps planners and decision-makers to obtain better real-world and less optimistic speed
36 predictions for their particular analysis.

37 The remainder of this paper is organized as follows. In the next chapter, we will briefly
38 stress on MFDs as a traffic analysis tool, define excess delays and outline the resampling approach
39 that we use to generate MFDs. In the following chapter, we will present three explorative ap-
40 proaches to fit an optimal speed curve to the resampled data sets. Thereafter, we will describe the
41 empirical data sets of five cities and the simulation data set. Then, we will present the results of
42 the analysis, and finish with a conclusion on our findings and policy implications.

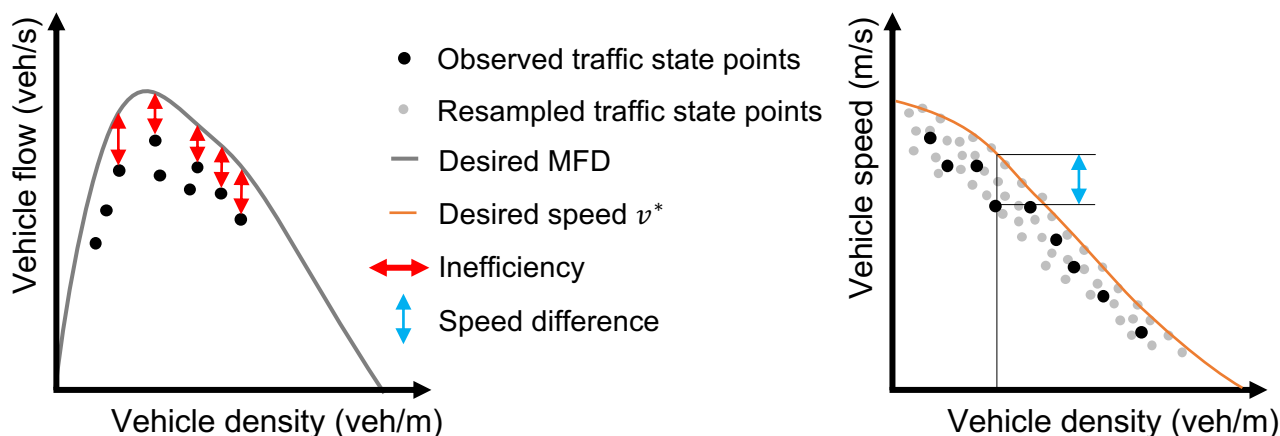


FIGURE 1 : Network inefficiency and estimating excess delays using the MFD.

1 METHOD

2 We quantify urban network inefficiency by the measure of *excess delays* based on the formulation
 3 of the MFD. As mentioned above, we define excess delays as those that exist in addition to the
 4 delays which can be derived by the idealized MFD for a given density. In the following subsections
 5 we discuss each building block in the process to calculate excess delays from MFD data.

6 The macroscopic fundamental diagram

7 The MFD describes the relationship between vehicle accumulation (density) and average traffic
 8 speed (or flow) in an urban road network (6). The general shape of the MFD can be seen in Figure 1.
 9 One can distinguish between the idealized or upper MFD (6, 8, 9) and the observed MFD (10, 11),
 10 both in the flow-density and in the speed-density relationship. The upper MFD represents the
 11 upper envelope to all possible states that are observed in the MFD. We define the optimal (desired)
 12 relationship between vehicle density, flow, and speed as the idealized MFD, which can be related
 13 to the social optimum. However, the desired speed-density relationship is rarely reached in reality
 14 and therefore difficult to measure. Delays in addition to the delays defined by the MFD then always
 15 occur when an observed data point does not match the desired speed-density relationship. In this
 16 paper, we will fit an upper speed MFD and derive an optimal speed-density relation by using a
 17 resampling approach (12). The resampling method is expected to result in less biased upper bound
 18 estimates with more supporting data (time span, experimental variation). If the underlying data
 19 is biased, e.g., only exhibiting one loading pattern, it could be that the resampled upper bound is
 20 biased in such a way that the excess delay estimation is less reliable in the sequel analysis. The
 21 MFD literature suggests that additional or *excess* delays occur for three main reasons:

- 22 1. **Multimodal vehicle interactions:** So far, most MFD literature focused on car traffic, al-
 23 though in the last years, interactions between different modes are receiving increasing atten-
 24 tion: For example, bi-modal interactions, i.e. between cars and buses (13, 14, 15) or cars
 25 and pedestrians (16), but also tri-modal interactions between cars, buses, and bicycles (17).
 26 As the latter show, interactions between different modes have different effects on the overall
 27 pace of the vehicles compared to cases where only unimodal interactions are considered.

1 Multimodal interaction effects come on top of the delays that occur due to network loading
2 and unloading (increasing and decreasing vehicle densities).

3 **2. Network loading processes and hysteresis:** Research has shown that the onset and offset
4 of congestion leads to different density distributions from a spatial perspective (18). This
5 is reflected in the MFD, where for a given density the observed flows during unloading of
6 the network, i.e. the offset of congestion, are usually lower than during the loading phase.
7 While the corresponding traffic dynamics can be explained by the FD on the link level, the
8 upper MFD curve fails to do so.

9 **3. Traffic signal control:** In some circumstances, the urban traffic controller may exert addi-
10 tional red times for car traffic, e.g. to protect a certain perimeter from overcrowding (19) or
11 to prioritize public transport (20). In either case, general traffic experiences additional delays
12 that are in excess to those that are reflected in the desired MFD.

13 Another contributor to excess delays could be the network topology and supply character-
14 istics, such as speed limits, lane widths, number of intersections, or its structure. For example, in a
15 city with a high number of links with speed limits below the city-wide speed limit, the mean speed
16 could be lower than average on the other links and therefore result in "artificial" excess delays. For
17 single analyses focusing on one city, this effect may be negligible. When comparing two different
18 cities with substantial differences in the network topology, we suggest controlling for these effects
19 in the delay model. This limitation will be further investigated in our future research, e.g., by sim-
20 ulation experiments that analyze the interaction effects of network structure and loading on excess
21 delays in particular.

22 **Network inefficiency based on excess delays**

23 Figure 1 shows where network inefficiency can be seen in the MFD. We define inefficiency as
24 the *gap* between the upper or desired MFD, and the observed traffic states in the flow-density
25 representation of the MFD. In the speed-density relationship, the gap can be directly translated
26 into an additional delay. Here, we express delay in the units of additional time per unit distance
27 (s/m). We quantify these additional delays in the following sequence. See Table 1 for the model
28 specification.

29 **1. Estimate the re-sampled MFD:** To approximate the smooth upper bound as good as pos-
30 sible that may correspond to the upper or desired speed MFD, we apply the re-sampling
31 method proposed by Ambühl et al. (12) on the aggregated data. The authors propose to ap-
32 ply sampling of representative subsets to generate the resampled data set. This procedure
33 aligns the data to more homogeneous distributions of network flow and density. Addition-
34 ally, it results in a smooth upper bound or boundary between observed and not observed
35 traffic states.

36 **2. Estimate the observed speed MFD:** The observed MFD from which v_{obs} is derived and for
37 which the delays γ are being calculated is estimated using the methods described in Leclercq
38 et al. (21) depending on the data source.

39 **3. Estimate the desired speed MFD v^* :** We estimate the upper or desired speed MFD, $v^*(k)$,
40 using the data from the re-sampled speed MFD and three different estimation methods to

TABLE 1 : Model specification

| Variable | Meaning |
|-----------|--|
| k | Average network density in vehicles per meter |
| v_{obs} | Average journey speed observed in the network in meters per second |
| v^* | Desired journey speed in the network in meters per second |
| γ | Excess delays in seconds per meter |
| L | Network loading indicator. Equals to one when network is in the loading state (increasing vehicle density), zero otherwise. Unitless |
| Parameter | Meaning |
| λ | MFD smoothing parameter (see (9)). Unitless |
| β_0 | Intercept of the excess delay model in seconds per meter |
| β_k | Effect of traffic density on excess delays in seconds per vehicle |
| β_L | Effect of network loading on excess delays in seconds per meter |

1 test for sensitivity of the relationships. More specifically, we fit in a quantile regression in
 2 the 99th percentile using (i) the functional form for the MFD proposed by [Ambühl et al. \(9\)](#)
 3 with the smoothing parameter λ ; (ii) the 99th percentile of the speed distribution at density
 4 bins and (iii) the exponential function proposed by [Underwood \(22\)](#) $v^*(k) = \exp(\log(c_0) +$
 5 $\log(c_1 * k))$.

6 **4. Estimate excess delays:** Finally, we calculate excess delays by $\gamma = 1/v_{obs} - 1/v^*$, where v^*
 7 is evaluated at the same density as observed for v_{obs} .

8 DATA

9 To enable an extended empirical comparison of excess delays and network inefficiency, we use
 10 traffic data from six European cities: Athens, Innsbruck, London, Lucerne, Paris, and Zurich. The
 11 cities are diverse, with large differences in e.g. surface areas, population size, network size, traffic
 12 densities, and average speeds. We chose two very large cities (> 1 million inhabitants), two mid-
 13 size cities (> 400.000 inhabitants) and two smaller cities (> 50.000 inhabitants) to test the method
 14 for different network scales. Also, the data collection methods for the data sets differ. Table 2
 15 shows an overview of the six data sets.

16 We first aggregate the data based on 2-minute time intervals for the Athens data set, and
 17 on 5-minute intervals for all other data sets, except for Paris. We chose a shorter time interval
 18 for Athens to generate a larger database. The aggregated data sets were used as base data for the
 19 resampling approach. Here, the number of randomly generated subsamples and the fraction size
 20 had to be specified. We chose a size of 100 subsamples and fraction sizes between 0.2 and 0.25. In
 21 other words, we resampled 20 to 25 percent of the aggregated data for each subsample (see Table
 22 2).

TABLE 2 : Overview of the traffic data sets from six European cities and the resampling(*) parameters

| Data set | Athens | Innsbruck | London | Lucerne | Paris | Zurich |
|---------------------------------|--------|------------|-----------|-----------|-----------|-----------|
| Population size (mil.) | 0.664 | 0.131 | 8.961 | 0.082 | 2.161 | 0.403 |
| Network size (km^2) | 1.3 | 33 | 160 | 5 | 24 | 15 |
| Detection method | drone | simulation | loop det. | loop det. | loop det. | loop det. |
| Time window | 4 days | 4 hours | 22 days | 365 days | 335 days | 365 days |
| Aggregation interval (seconds)* | 120 | 300 | 300 | 300 | 3600 | 300 |
| No. of subsamples* | 100 | 100 | 20 | 100 | 20 | 100 |
| Fraction size (in %)* | 0.25 | 0.25 | 0.2 | 0.25 | 0.2 | 0.25 |

1 **Loop detector data: Lucerne, London, Paris, Zurich**

2 The data of Lucerne, Zurich, London, and Paris is part of the UTD19 dataset (23, 24). The large-
3 scale traffic data was assembled through stationary loop detectors in the city areas. Loop detectors
4 measure the occupancy, i.e. the time fraction that a vehicle occupies a detector, and the traffic
5 count, i.e., the number of vehicles passing the detector, for a fixed time interval. In Lucerne and
6 Zurich, data was collected over a time period of a year. In London and Paris, data was collected
7 over 22 and 335 days, respectively. We selected all observations during the daytime, between
8 6 a.m. and 8 p.m. The Paris data set is aggregated on a time interval of an hour, as the loop
9 detector only generates observations in this frequency. The other three data sets are aggregated in
10 intervals of 5 minutes. The loop detector data differs from the pNEUMA data set and Innsbruck
11 simulation data with the former covering the morning hours only and the latter simulating four
12 hours of weekday traffic.

13 **Drone data: Athens**

14 The observations of the data set pNEUMA (25) were collected by ten drones flying over the cen-
15 tral business district of Athens, Greece, during the morning hours. The data contains the latitude
16 and longitude values for different vehicle types, namely car, bus, motorcycle, medium and heavy
17 vehicles, and taxis over time fractions of 0.04 seconds. The number of observations for pNEUMA
18 is smaller compared to the detector-based UTD-datasets, as the measurement period comprised 4
19 weekdays only. Because the observations of some drone flights indicated measurement errors, the
20 preprocessing was extensive. For example, we removed the eighth drone flight and the observa-
21 tions of the last 2 minutes of every drone flight, as the reported speeds and densities indicate that
22 there might be measurements errors. To derive density values from the data set, we assumed a
23 network length of 100 km according to the official data set description. Finally, we aggregated the
24 observations in 2-minute intervals.

1 **Simulation data: Innsbruck**

2 The Innsbruck data was generated with a microscopic traffic simulation using SUMO (26). The
3 network was retrieved from OpenStreetMaps (27). For all included traffic behavior models, the
4 default parameters were chosen. Thus, the simulation is not calibrated. However, for the current
5 study, such a calibration is not essential as we investigate traffic flow dynamics and their effects on
6 the network level. Such mechanisms are included in the simulation due to the physical modeling
7 of driving behavior.

8 The origin-destination patterns were randomly generated. The loading curve has a trape-
9 zoidal shape, i.e. after a step-wise loading, the maximum demand was kept for some time intervals,
10 until the demand was decreased again in a step-wise manner. Such loading curves are commonly
11 applied to mimic a rush-hour including its onset and offset. The loading and unloading phase lasted
12 for 1.5 [h] each, the plateau phase for 1 [h], which results in a total simulation time of $T = 4$ [h].

13 Vehicles follow the shortest path from their origin to their destination. In the simulation,
14 we apply a quasi-dynamic traffic assignment, where the shortest paths are updated for all vehicles
15 considering the current traffic states in the network for every 2 minutes. In other words, all vehicles
16 can adapt their route before they reach their destination if such a change is of advantage. Such an
17 assignment represents a reasonable trade-off between realism and computational cost (28).

18 To allow the analysis of the impact of signal control on the network inefficiency, we varied
19 the signal control parameters. We assume that all traffic signals follow a fixed-time control logic,
20 have a common cycle length, have the same green-to-cycle ratio of 0.5, and no offsets apply. Three
21 different cases with a cycle length of 60, 90, and 120 [s] were investigated. Previous research has
22 shown that offsets do not have a major impact on the resulting MFD (29).

23 **RESULTS**

24 The resampling method proved successful to build the upper bound of the MFD for all six data sets.
25 As expected, we obtain a decreasing non-linear speed-density relation for all cities (see Figure 2).
26 We see that the range of vehicle density is higher for London, Lucerne, Paris, and Zurich than for
27 Innsbruck and Athens. Not surprisingly, the larger data sets show less scatter than the smaller ones
28 (Athens, Innsbruck). For the latter, the resampling method proves especially useful as it generates
29 a more reliable database. In Figure 2, we obtain for every estimation method (Ambühl (9), the
30 percentile approach, and Underwood (22)) the optimal speed curves v^* for all six data sets. We
31 find that all three fitting methods for v^* obtain comparable relationships. Eventually, differences
32 can be explained by the estimation methods, e.g. a limited flexibility due to functional assumptions
33 in the Underwood and Ambühl case. With substantial observations and scatter in the uncongested
34 regime and less in the congested regime, these two functions, which weigh each point equally in
35 the estimation, have to balance these differences. This leads to a relationship that appears to be
36 below the upper MFD in the uncongested regime, while better describing the upper MFD in the
37 congested regime. This has implications for the estimation of excess delays that can be less reliable
38 in the uncongested regime.

39 Based on the fitted optimal speed curves from Figure 2, we examined the relationship be-
40 tween excess delays and densities. The kernel density estimates of delays on the right-hand side of
41 Figure 3 show the frequency of the delay value range, calculated with Underwoods' method. As
42 expected, Athens and Innsbruck show more variance in the excess delay distribution as the database
43 is small. The UTD-data sets approach a Gaussian bell shape, especially Lucerne and Zurich, being
44 the largest data sets. Athens, Innsbruck, and Zurich have a mean excess delay of approximately

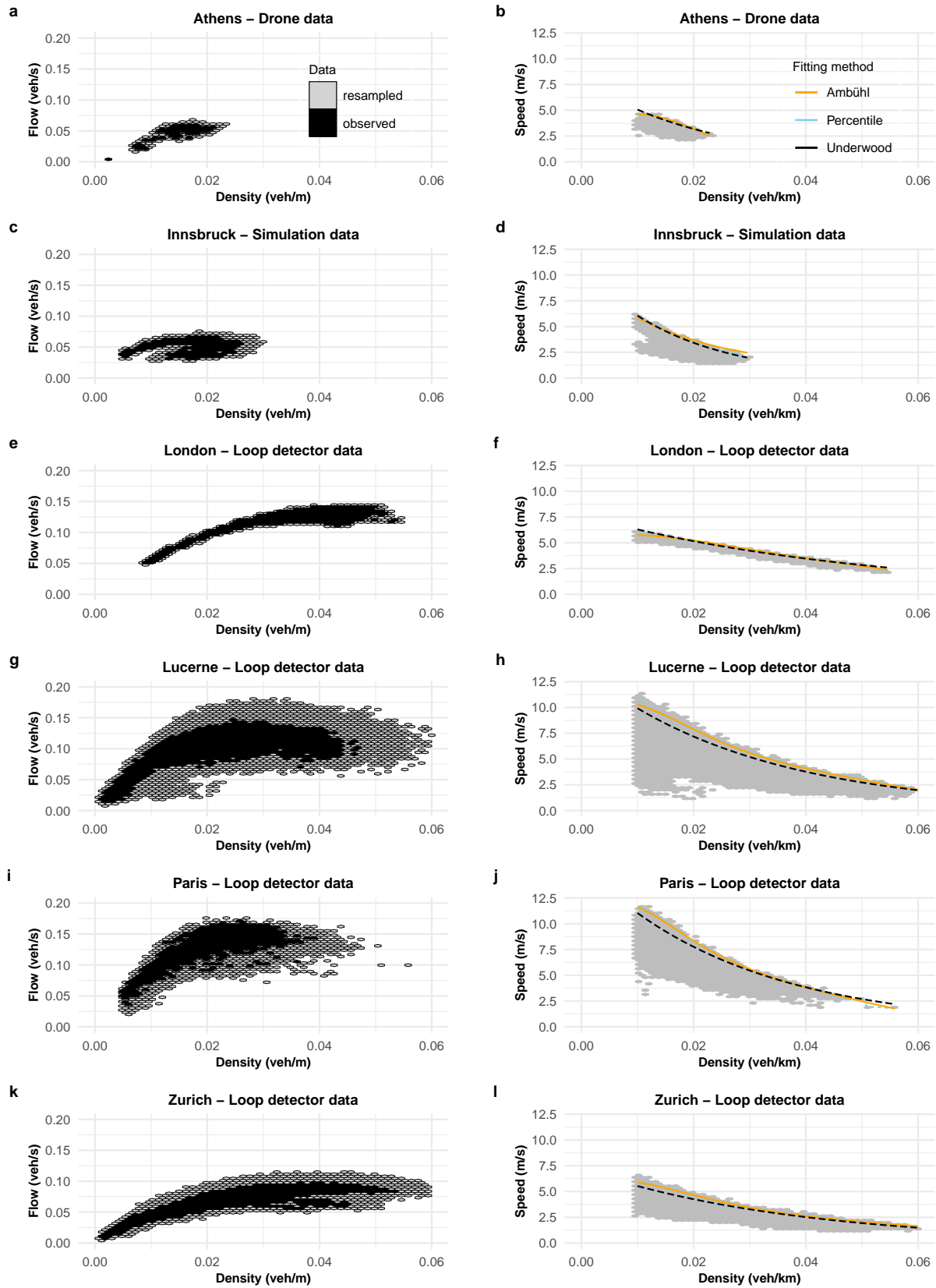


FIGURE 2 : Desired flow-density (left) and speed-density (right) MFDs and three fitting methods for v^* for six cities.

1 0.05 to 0.06 seconds per meter. London, Lucerne, and Paris have a mean excess delay of approxi-
2 mately 0.02 to 0.03 seconds per meter. As can be seen in Figure 3, we obtain positive relationships
3 between higher vehicle densities and excess delays, especially in higher density ranges, for Inns-
4 bruck, London, Lucerne, and Zurich. This indicates that v^* is less likely obtained, the more density
5 is observed in an urban road network. The plotted results indicate that the estimation methods do
6 not differ considerably.

7 **Network loading**

8 To test the influence of network loading and unloading process on the development of excess
9 delays, we derive from the data an indicator variable L that equals one if the network is loading
10 and zero otherwise. We assume that the network is in a loading state when the difference in
11 density of two consecutive intervals is positive, after applying a three-interval moving average on
12 the density to reduce the noise in the data. We then estimated a linear regression to analyze the
13 effect of density k and slope L on excess delays γ . We estimate the linear model as given in Eqn.
14 1, where β_0 , β_k and β_L are parameters to be estimated using ordinary least squares. ε represents
15 the error terms that are assumed to be normally distributed.

$$\gamma = \beta_0 + \beta_k \cdot k + \beta_L \cdot L + \varepsilon \quad (1)$$

16 As the excess delay values and relationships that result from the three v^* fitting approaches
17 look very similar (see Figure 2), we present the results only for the Underwood model in Table
18 3. The results for the other three models do not alter the findings. Generally, we find that the
19 model formulated in Eqn. 1 explains substantial variance found in Athens, Innsbruck, London,
20 and Lucerne. The low R^2 in Paris and Zurich suggests that the model does not well describe
21 the data for these cities. Potentially, the value for Paris results from the temporal aggregation at
22 one-hour intervals instead of 2-5 minute intervals, where many of the dynamic effects might be
23 averaged out. In future research, we will investigate further the factors of the distribution of excess
24 delays in Paris and Zurich.

25 For Athens, Innsbruck, London, Lucerne, and Zurich we find positive and statistically sig-
26 nificant effects of vehicle density on excess delays. However, their effect sizes differ by one order
27 magnitude. Future research has to investigate why this effect is so substantially different between
28 the shown networks. Potential reasons are data bias, network topology, traffic control, etc. In ad-
29 dition, Figure 4 for Innsbruck suggests that the linear model in Eqn. 1 is falsely specified as the
30 loading and unloading effect and their interaction are clearly not linear. This means that the model
31 formulation from Eqn. 1 might not capture all underlying mechanisms, which could be a reason
32 for the alternate effect direction found in Paris. Here, the effect estimation regarding the loading
33 part results in $\beta_k = 0.377$ ($p < 0.01$), which supports the findings related to the other five cities. The
34 effect corresponds to increasing excess delays with traffic density. More specifically, we observe
35 an increase of the estimates around 1 s/m for every 0.01 veh/m increase. Note that this effect is in
36 addition to the speed reduction already captured in the MFD. Nevertheless, the findings from Paris
37 indicate that an analysis of the differences could reveal further insights.

38 The six cities cover different spatial scales to understand the behavior of the loading indica-
39 tor for different city sizes. The indicator variable for loading is negative and statistically significant
40 in Athens, Innsbruck, Lucerne, and Zurich, while Zurich and Lucerne report an effect of one order
41 of magnitude less than Athens and Innsbruck. It means that during the network loading, fewer ex-

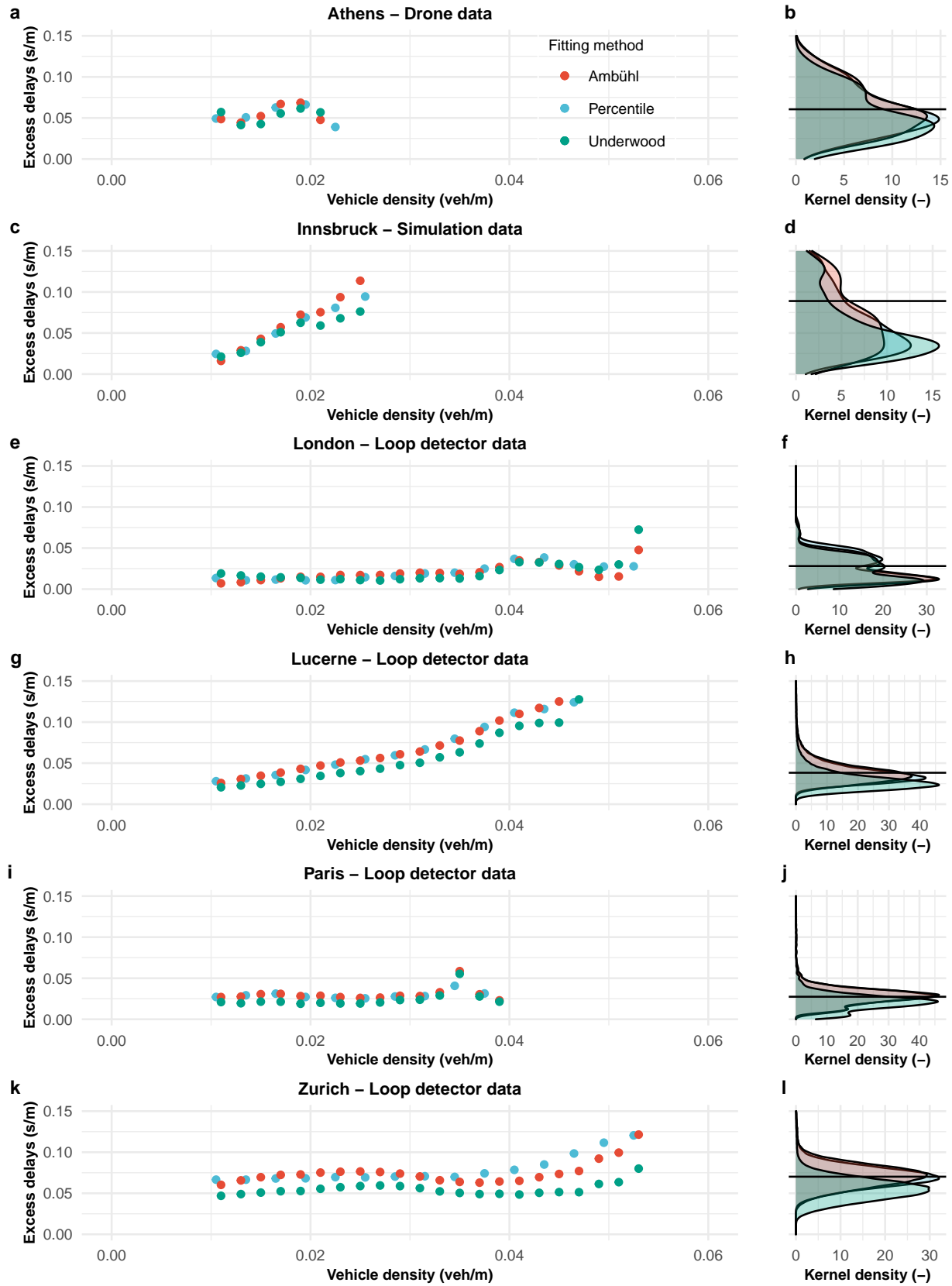


FIGURE 3 : Relationship between vehicle density and excess delays (left), and kernel densities (right), for each fitting method.

TABLE 3 : Model estimation results for excess delays.

| Dataset | Effect of density | Effect of loading | R^2 | Density range (veh/m) |
|-----------|-------------------|-------------------|-------|-----------------------|
| Athens | 2.96 (p < 0.01) | -0.038 (p < 0.01) | 0.26 | 0.01 to 0.02 |
| Innsbruck | 3.53 (p < 0.01) | -0.090 (p < 0.01) | 0.53 | 0.01 to 0.03 |
| London | 1.13 (p < 0.01) | 0.001 (p < 0.01) | 0.19 | > 0.02 |
| Lucerne | 2.30 (p < 0.01) | -0.003 (p < 0.01) | 0.30 | > 0.02 |
| Paris | -0.24 (p < 0.05) | 0.001 (p < 0.01) | 0.006 | > 0.02 |
| Zurich | 0.48 (p < 0.01) | -0.002 (p < 0.01) | 0.03 | > 0.02 |

cess delays are present compared to the unloading, e.g. supporting the development of hysteresis in the MFD. The positive effect in London and Paris deserves more attention, especially from an econometric perspective. In the model specification from Eqn. 1, there are no control variables included. Consequently, any factor that could contribute to excess delays and that correlates either with traffic density or the loading indicator variable is partially included in the estimated effect. As the model is estimated for the entire urban area in London and Paris, this could be an increase in bus services during the loading phase that increases excess delays (30), a gating traffic control scheme that increases red phases for inbound traffic to protect the urban core from gridlock which adds waiting time and thus increases excess delays (19), or any origin-destination-based effect. Consequently, future research should improve the estimates with more detailed model formulations.

12 Traffic control

13 The simulation of Innsbruck enables to vary signal control parameters and study corresponding effects on the excess delay. For this purpose, we investigate three different scenarios, where the cycle length of all signals equals 60, 90, and 120 seconds. Figure 4 shows the resulting scatter plot for the loading and unloading part of the MFD as well as a local polynomial regression fitting (loss) of R's ggplot package to investigate the trend in the data.

18 For all three scenarios, we observe the already revealed positive relationship between vehicle density and excess delays in the loading part. In the unloading part, we see that excess delays are decreasing with vehicle density, hinting towards a clockwise hysteresis. Importantly, the data suggest that differences in the relationship between different traffic signal settings and excess delays exist. The influence seems to be nonlinear concerning the cycle length as the trend lines do not appear in ascending or descending order, but in the sequence 90, 120, and 60 seconds. This confirms that traffic control indeed has not only an effect on inherent delays already included in the MFD, but indeed also on excess delays as suggested in this paper. The impact of cycle times seems to be larger in the unloading part compared to the loading part as it can be seen in Figure 4. However, in future research, we will investigate this relationship more extensively using more simulation scenarios.

29 Note that the apparent relationship between excess delay and density in Figure 4 in the unloading part suggests that simple mathematical modeling of hysteresis effects is possible. This will be further explored in future research.

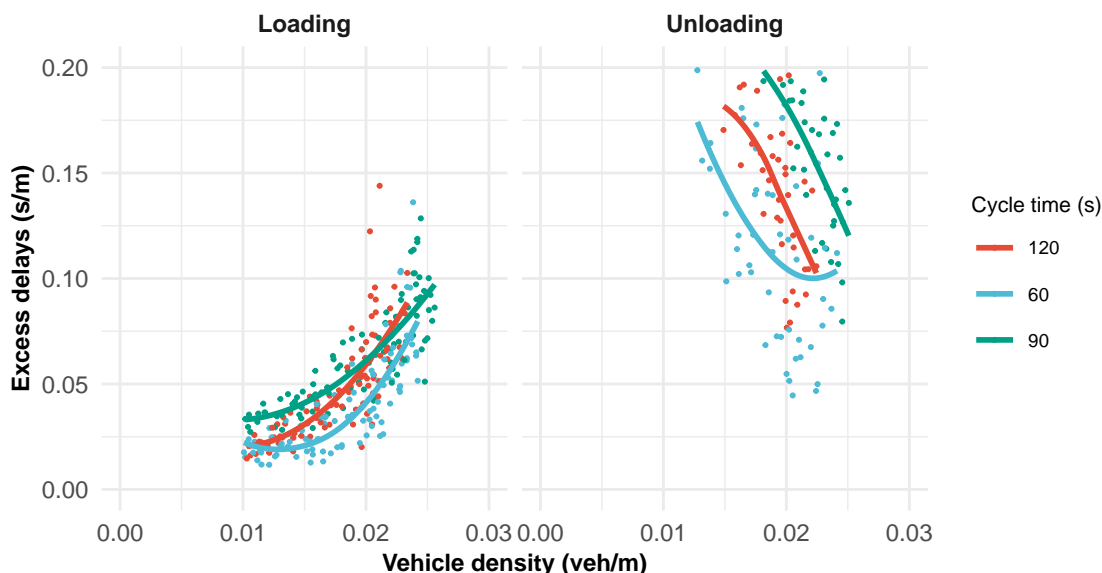


FIGURE 4 : Influence of cycle lengths on excess delays using the Innsbruck simulation data.

1 Multimodal traffic in Athens

2 We further investigate the variation of excess delays in Athens by distinguishing between different
 3 vehicle types. We use the pNEUMA data here, as it is the only data set allowing such in-depth mul-
 4 timodal analyses. Note that there exists already a paper on multi-modal interactions at space-mean
 5 network speed working with the pNEUMA data set (31). The authors use regression models of
 6 the space-mean speed on the vehicle accumulations of the multimodal traffic. The core distinction
 7 of the analysis presented in this paper is that we do not use a speed-accumulation relationship but
 8 an excess delay formulation, i.e., additional time delay in s/m in relation to the maximum speed
 9 at a given density. In each time interval, we compute the share of taxis, large vehicles (labeled as
 10 'large and medium-sized vehicles' in the original data), buses, and motorcycles. Figure 5 shows
 11 the resulting scatter plots. For the share of taxis, large vehicles and motorcycles we find a posi-
 12 tive relationship with excess delays, while for the share of buses we find a negative relationship.
 13 This seems perhaps surprising given that the 3D-MFD assumes negative interaction costs between
 14 cars and buses (13). To explore the multivariate nature of the data, we estimate a linear model
 15 of excess delays as a function of the taxi, large vehicle, bus, and motorcycle share. We find sta-
 16 tistically significant (1 % level) marginal effects of taxi share of 0.39 (s/m), and truck share of
 17 0.62 (s/m). This means that when the taxi share increases by ten percentage points, excess delays
 18 increase by 0.04 (s/m). This can be translated to an additional delay of 3.3 minutes for a typical
 19 journey with a length of 5 km per 10 % taxi share increase. When the large vehicle share increases
 20 by ten percentage points, excess delays increase by 0.06 (s/m). For buses, the model estimate of
 21 -1.37 (s/m) (statistically significant at 1 % level) confirms the relationship from Figure 5. This
 22 counter-intuitive relationship may result from the limited sample size and experimental variation:
 23 The share of buses correlates strongly negatively with vehicle density. In other words, the share of
 24 buses only increases as a consequence of an overall decreasing vehicle density (fixed timetable).
 25 Thus, this variable approximates more high and low demand traffic states and less the impact of
 26 buses. This makes the revealed estimate reasonable. Nevertheless, this finding emphasizes that an

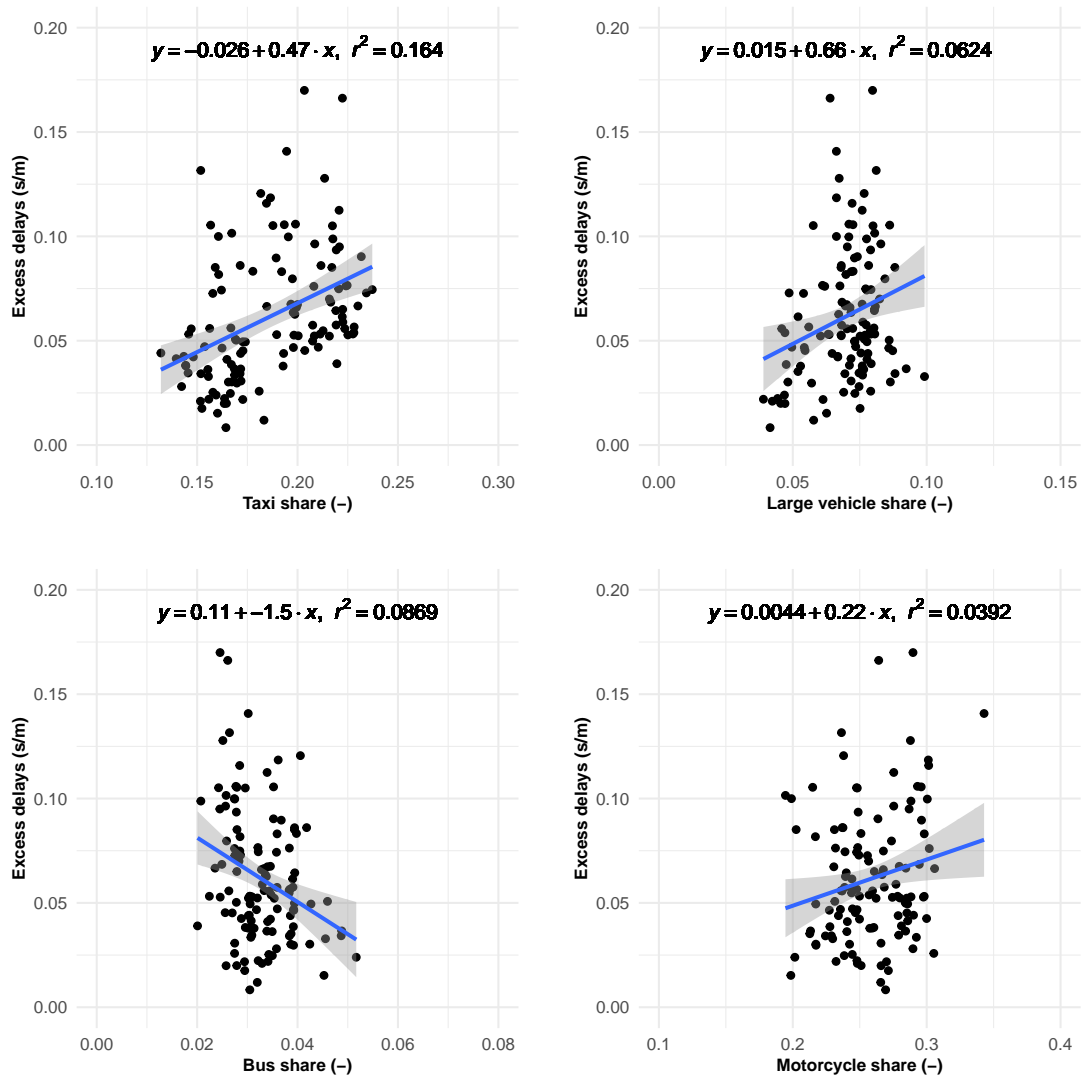


FIGURE 5 : The influence of multimodal traffic on excess delays in Athens.

1 important variable is omitted in the present model formulation. The model does not reveal a sta-
2 tistically significant effect of motorcycles, i.e. the relationship found in Figure 5 is not supported.
3 Overall, the model has a goodness of fit of $R^2 = 0.27$, when controlling for potential outliers it
4 increases to $R^2 = 0.37$.

5 Multi-modal traffic occurs in all cities including the resulting interaction effects. In larger
6 cities such as Paris or London, the flows of bicycles and scooters are clearly observable and are
7 quite likely contributing to excess delays. To account for them in the excess delay formulation,
8 many observations and sufficient experimental variation are required (high/low volumes of cars
9 and high/low volumes of bicycles or scooters) to reveal the interaction effects shown in field ex-
10 periments (17, 32). Another modeling challenge is the violation of traffic regulations, which might
11 impede the observation and estimation of effects. In the case of the pNEUMA data set, the exper-
12 imental variation was limited, leading to a high correlation of densities and the expected effects
13 could not be revealed. In cities with loop detector data, one approach to control for the impact
14 of bicycles/scooters on excess delays would be to use bicycle counts from permanent counting
15 locations as a proxy. Unfortunately, such data was not available to the authors.

16 CONCLUSION

17 In this paper, we showed that urban road networks experience substantial inefficiencies as seen in
18 the presence of excess delays. We defined excess delays as the difference between the optimal and
19 observed pace. Using five empirical data sets (loop detector and drone data) from European cities
20 and one simulation data set, we observed network inefficiencies in every city. Even though the
21 extent of excess delays differs across cities, their general effects and evolution are highly similar.
22 This supports the applicability of the method for other cities. We further investigated causes for
23 the emergence of excess delays, which would make them predictable: (i) network loading, causing
24 inherent delays produced by increasing density (ii) signal control, which we showed for different
25 cycle lengths in Innsbruck and (iii) multimodal interaction effects between different vehicle types,
26 supported by data from multimodal traffic data set of Athens. Regarding (i), the results of the delay-
27 density relation for the Innsbruck data suggest that our approach might simplify the mathematical
28 modeling of hysteresis effects.

29 With this paper, we not only contribute to improved modeling of the evolution of congestion
30 in cities at the network level but also to a more realistic capacity planning for urban road networks.
31 We show that there exists an optimal, achievable speed curve for large, medium-sized, and small
32 cities. We also demonstrate that the proposed method applies to different forms of data sets - loop
33 detector data, drone data, and simulation data. The inefficiency of excess delays can be measured
34 easily by the proposed methods and only requires average speed and density values for a given area
35 and time period. To find out which factors affect excess delays, it would be suitable to compare
36 the measured excess delays of a specific area in a city for a given time period with a simulation of
37 this respective scenario. Then, measures could be derived to reduce the effects on excess delays
38 and therefore minimize speed drop.

39 The practical implications of this paper primarily concern the applications of the proposed
40 approach. First, it helps to identify and quantify factors on excess delays in a city more conve-
41 niently compared to modeling speeds directly - either using empirical data or simulation experi-
42 ments. Then, measures (design features, traffic management) could be derived to reduce excess
43 delays and therefore minimize speed and accessibility losses either by scenario analysis or by
44 a cross-sectional analysis of several cities. Second, applications of the proposed network inef-

1 efficiency approach can be possible everywhere in the field of network-wide traffic management
2 where an improved capacity and speed estimate is valued for improved traffic and economic out-
3 comes, e.g., road pricing or perimeter control. Third, the proposed method can be applied as a
4 performance indicator to assess the impact of time and space allocation in an urban network: In
5 those areas or hours with a high share of excess delays, traffic could be allocated to other roads
6 or shifted to other time periods, e.g., through intelligent passenger information systems. As the
7 optimal speed v^* is almost never reached in real-world scenarios, network planners might create
8 more space and capacity to obtain the optimal speed for cars. This is difficult to realize, e.g. due
9 to limited space in urban areas and the risk of induced traffic. Multimodal system improvement
10 in combination with setting up mode-independent accessibility values (for example, by measuring
11 the minimum required transport speed or maximum acceptable travel time) which have to be met
12 by a traffic system, could be a possible solution.

13 This paper introduces and discusses the idea of measuring network inefficiency by the
14 concept of excess delays. Therefore, there are limitations to the study and opportunities for future
15 research. First, we did not consider at the present stage the influence of structural network effects,
16 e.g. speed limits or network design, on the evolution of excess delays. As the MFD is governed
17 by network topology, one could argue that it influences excess delays too. Second, the fitting of
18 v^* to identify the upper MFD can be improved as the relationships do not perfectly match the re-
19 sampled upper MFD, e.g. by weighting observations. Only when we can correctly describe the
20 upper MFD, we can retain unbiased excess delay estimates that are important for further modeling.
21 This also requires a throughout data filtering and unbiased MFD estimation prior to the derivation
22 of excess delays. Once unbiased excess delays estimates are retrieved, we can follow on the first
23 evidence present on its driving factors (network loading, signal control, and multimodality) to
24 improve the estimates and, using more extensive experiments (empirical data, simulation), obtain
25 global validity of these estimates.

26 In closing, describing network inefficiency by excess delays seems to be promising because
27 it makes the former predictable. As effect sizes are similar, too, across cities in our study, we are
28 convinced that the revealed effects can be found in every city. Last, we consider that using drone
29 data for calibrating a city's multimodal excess delays effects is promising, as it allows quantifying
30 otherwise unobserved factors.

31 ACKNOWLEDGEMENTS

32 Lisa S. Hamm acknowledges support from the German Federal Ministry of Transport and Digital
33 Infrastructure (BMVI) for the funding of the project TEMPUS (Test Field Munich - Pilot Test
34 Urban Automated Road Traffic). Allister Loder acknowledges support from the German Federal
35 Ministry of Transport and Digital Infrastructure (BMVI) for the funding of the project KIVI (Ar-
36 tificial Intelligence in Ingolstadt's Transportation System), grant no. 45KI05A011. Gabriel Tilg
37 acknowledges support from the German Federal Ministry of Transport and Digital Infrastructure
38 (BMVI) for the funding of the project LSS (Capacity increase of urban networks). Monica Menen-
39 dez acknowledges the support from the NYUAD Center for Interacting Urban Networks (CITIES),
40 funded by Tamkeen under the NYUAD Research Institute Award CG001 and by the Swiss Re In-
41 stitute under the Quantum Cities™ initiative. As a data source, the pNEUMA data set was used:
42 open-traffic.epfl.ch

1 AUTHOR CONTRIBUTIONS

2 The authors confirm contribution to the paper as follows: L. Hamm, A. Loder contributed to the
3 study conception and design, and model design. L. Hamm, A. Loder, G. Tilg, M. Menendez
4 contributed to the draft manuscript preparation, and the results analysis and interpretation. All
5 authors reviewed the results and approved the final version of the manuscript.

6 References

- 7 1. Bai, L., S. Wong, P. Xu, A. H. Chow, and W. H. Lam, Calibration of stochastic link-based fun-
8 damental diagram with explicit consideration of speed heterogeneity. *Transportation Research*
9 *Part B: Methodological*, Vol. 150, 2021, pp. 524–539.
- 10 2. Buisson, C. and C. Ladier, Exploring the impact of homogeneity of traffic measurements on
11 the existence of macroscopic fundamental diagrams. *Transportation Research Record*, Vol.
12 2124, No. 1, 2009, pp. 127–136.
- 13 3. Mazlounian, A., N. Geroliminis, and D. Helbing, The spatial variability of vehicle densities
14 as determinant of urban network capacity. *Philosophical Transactions of the Royal Society A:*
15 *Mathematical, Physical and Engineering Sciences*, Vol. 368, No. 1928, 2010, pp. 4627–4647.
- 16 4. Geroliminis, N. and J. Sun, Properties of a well-defined macroscopic fundamental diagram
17 for urban traffic. *Transportation Research Part B: Methodological*, Vol. 45, No. 3, 2011, pp.
18 605–617.
- 19 5. Knoop, V. L., H. Van Lint, and S. P. Hoogendoorn, Traffic dynamics: Its impact on the macro-
20 scopic fundamental diagram. *Physica A: Statistical Mechanics and its Applications*, Vol. 438,
21 2015, pp. 236–250.
- 22 6. Daganzo, C. F., Urban gridlock: Macroscopic modeling and mitigation approaches. *Trans-*
23 *portation Research Part B: Methodological*, Vol. 41, No. 1, 2007, pp. 49–62.
- 24 7. Geroliminis, N. and C. F. Daganzo, Existence of urban-scale macroscopic fundamental
25 diagrams: Some experimental findings. *Transportation Research Part B: Methodological*,
26 Vol. 42, No. 9, 2008, pp. 759–770.
- 27 8. Daganzo, C. F., L. J. Lehe, and J. Argote-Cabanero, Adaptive offsets for signalized streets.
28 *Transportation Research Part B: Methodological*, Vol. 117, 2018, pp. 926–934.
- 29 9. Ambühl, L., A. Loder, M. C. Bliemer, M. Menendez, and K. W. Axhausen, A functional form
30 with a physical meaning for the macroscopic fundamental diagram. *Transportation Research*
31 *Part B: Methodological*, Vol. 137, 2020, pp. 119–132.
- 32 10. Ambühl, L., A. Loder, L. Leclercq, and M. Menendez, Disentangling the city traffic rhythms:
33 A longitudinal analysis of MFD patterns over a year. *Transportation Research Part C: Emerg-*
34 *ing Technologies*, Vol. 126, 2021, p. 103065.
- 35 11. Tilg, G., L. Ambühl, S. Batista, M. Menendez, L. Leclercq, and F. Busch, Semi-analytical es-
36 timation of macroscopic fundamental diagrams: from corridors to networks. In *100th Annual*
37 *Meeting of the TRB*, 2021.
- 38 12. Ambühl, L., A. Loder, M. Bliemer, M. Menendez, and K. Axhausen, Introducing a re-
39 sampling methodology for the estimation of empirical macroscopic fundamental diagrams.
40 *Transportation Research Record*, Vol. 2672, No. 20, 2018.
- 41 13. Geroliminis, N., N. Zheng, and K. Ampountolas, A three-dimensional macroscopic fundamen-
42 tal diagram for mixed bi-modal urban networks. *Transportation Research Part C: Emerging*
43 *Technologies*, Vol. 42, 2014, pp. 168–181.
- 44 14. Dakic, I., L. Ambühl, O. Schümperlin, and M. Menendez, On the modeling of passenger

- 1 mobility for stochastic bi-modal urban corridors. *Transportation Research Part C: Emerging*
- 2 *Technologies*, Vol. 113, 2020, pp. 146–163.
- 3 15. Tilg, G., Z. Ul Abedin, S. Amini, and F. Busch, Simulation-based design of urban bi-modal
- 4 transport systems. *Frontiers in Future Transportation*, Vol. 1, 2020.
- 5 16. Daganzo, C. F. and V. L. Knoop, Traffic flow on pedestrianized streets. *Transportation Re-*
- 6 *search Part B: Methodological*, Vol. 86, 2016, pp. 211–222.
- 7 17. Loder, A., L. Bressan, M. J. Wierbos, H. Becker, A. Emmonds, M. Obee, V. L. Knoop,
- 8 M. Menendez, K. W. Axhausen, and A. Loder, How Many Cars in the City Are Too Many
- 9 ? Towards Finding the Optimal Modal Split for a Multi-Modal Urban Road Network. *Fron-*
- 10 *tiers in Future Transportation*, Vol. 2, No. May, 2021.
- 11 18. Gayah, V. V. and C. F. Daganzo, Clockwise hysteresis loops in the macroscopic fundamental
- 12 diagram: An effect of network instability. *Transportation Research Part B: Methodological*,
- 13 Vol. 45, 2011, pp. 643–655.
- 14 19. Geroliminis, N., J. Haddad, and M. Ramezani, Optimal Perimeter Control for Two Urban Re-
- 15 gions With Macroscopic Fundamental Diagrams: A Model Predictive Approach. *IEEE Trans-*
- 16 *actions on Intelligent Transportation Systems*, Vol. 14, No. 1, 2013, pp. 348–359.
- 17 20. Guler, S. I. and M. Menendez, Analytical formulation and empirical evaluation of pre-signals
- 18 for bus priority. *Transportation Research Part B: Methodological*, Vol. 64, 2014, pp. 41–53.
- 19 21. Leclercq, L., N. Chiabaut, and B. Trinquier, Macroscopic fundamental diagrams: A cross-
- 20 comparison of estimation methods. *Transportation Research Part B: Methodological*, Vol. 62,
- 21 2014, pp. 1–12.
- 22 22. Underwood, R. T., Speed, Volume and density relationships. In *Quality and Theory of Traffic*
- 23 *Flow*, Pennsylvania State University, University Park, 1961, pp. 141–188.
- 24 23. Loder, A., L. Ambühl, M. Menendez, and K. W. Axhausen, *UTD19. Understanding traffic*
- 25 *capacity of urban networks*. Zurich, 2020-08.
- 26 24. Loder, A., L. Ambühl, M. Menendez, and K. W. Axhausen, Understanding traffic capacity of
- 27 urban networks. *Scientific Reports*, Vol. 9, No. 1, 2019, p. 16283.
- 28 25. Barmounakis, E. and N. Geroliminis, On the new era of urban traffic monitoring with mas-
- 29 sive drone data: The pNEUMA large-scale field experiment. *Transportation Research Part C:*
- 30 *Emerging Technologies*, Vol. 111, No. November 2019, 2020, pp. 50–71.
- 31 26. Lopez, P. A., M. Behrisch, L. Bieker-Walz, J. Erdmann, Y.-P. Flötteröd, R. Hilbrich,
- 32 L. Lücken, J. Rummel, P. Wagner, and E. Wießner, Microscopic traffic simulation using
- 33 SUMO. In *The 21st IEEE International Conference on Intelligent Transportation Systems*,
- 34 IEEE, 2018.
- 35 27. OpenStreetMap contributors, *Innsbruck dump* retrieved from <https://planet.osm.org> , 2020.
- 36 28. Mühlich, N., V. V. Gayah, and M. Menendez, Use of Microsimulation for Examination of
- 37 Macroscopic Fundamental Diagram Hysteresis Patterns for Hierarchical Urban Street Net-
- 38 works. *Transportation Research Record*, Vol. 2491, No. 1, 2015, pp. 117–126.
- 39 29. Girault, J.-T., V. V. Gayah, I. Guler, and M. Menendez, Exploratory analysis of signal co-
- 40 ordination impacts on macroscopic fundamental diagram. *Transportation Research Record:*
- 41 *Journal of the Transportation Research Board*, Vol. 2560, No. 2560, 2016, pp. 36–46.
- 42 30. Loder, A., L. Ambühl, M. Menendez, and K. W. Axhausen, Empirics of multi-modal traffic
- 43 networks – Using the 3D macroscopic fundamental diagram. *Transportation Research Part C:*
- 44 *Emerging Technologies*, Vol. 82, 2017, pp. 88–101.
- 45 31. Paipuri, M., E. Barmounakis, N. Geroliminis, and L. Leclercq, Empirical observations of

- 1 multi-modal network-level models: Insights from the pNEUMA experiment. *Transportation*
2 *Research Part C: Emerging Technologies*, Vol. 131, 2021, p. 103300.
- 3 32. Wierbos, M. J., V. L. Knoop, F. S. Hänseler, and S. P. Hoogendoorn, A macroscopic flow
4 model for mixed bicycle–car traffic. *Transportmetrica A: Transport Science*, Vol. 17, No. 3,
5 2021, pp. 340–355.